Intravenous administration-oriented pharmacokinetic model for dynamic bioluminescence imaging

Yunpeng Dai, Guodong Wang, Duofang Chen, Jipeng Yin, Yonghua Zhan, Yongzhan Nie, Kaichun Wu, Jimin Liang*, Xueli Chen*, *Member, IEEE*

***Abstract*—*Objective*: *In vivo* bioluminescence imaging (BLI) is a promising tool for monitoring the growth and metastasis of tumors. However, quantitative BLI research based on intravenous (IV) injection is limited, which greatly restricts its further application. To address this problem, we designed a pharmacokinetic (PK) model which is suitable for applying on IV administration of small amounts of D-Luciferin. *Methods*: After three weeks of post-implantation, mkn28-luc xenografted mice were subjected to 40 min dynamic BLI immediately following D-Luciferin intravenous injection on days 1, 3, 5, 7 and 9. Further, the PK model was applied on dynamic BLI data to obtain the sum of kinetic rate constants (SKRC). *Results*: Results showed that the SKRC values decreased rapidly with the growth of the tumor. There was a statistical difference between the SKRC values measured at different time points, while the time point of luminous intensity peak (TLP) was unaffected by the growth of the tumor. *Conclusions*: In short, our results imply that dynamic BLI combined with our PK model can predict tumor growth earlier and with higher sensitivity compared to the conventional method, which is crucial for improving drug evaluation efficacy. In addition, the dynamic BLI may provide a valuable reference for the noninvasive acquiring arterial input function (AIF), which may also provide a new application prospect for hybrid PET-optical imaging.**

***Index Terms*—Biomedical optical imaging, Medical diagnostic imaging, Molecular imaging, Biological system modeling.**

I. Introduction

BIOLUMINESCENCE imaging (BLI) is a technology that detects luminescence that can only be obtained by biological biochemical reactions, and does not require exogenous excitation [1-3]. Similar to fluorescence imaging (FI), it can also be used for real-time and non-invasive imaging of biochemical processes *in vivo* [4]. Because the spontaneous luminous intensity of the organism itself is very weak, a satisfactory image signal-to-noise ratio can be obtained by BLI [5]. Another advantage of BLI over FI is that it can detect fluorescein substrates with shorter luminous half-life, which can be decomposed in a short period of time [6]. Thus, under BLI the normal biochemical processes of the organism are not unduly disturbed, which provides the appropriate conditions for longitudinal studies requiring continuous observations [7]. For example, Sim *et al.* presented a quantitative analysis of tumor growth based on the intraperitoneal injection of D-luciferin [8]. In their study, a 2-compartment PK model was used to obtain kinetic parameters that can accurately describe and replicate the biodistribution of luciferin and the growth kinetics of tumors. However, so far most of the studies have been based on static BLI. In particular, quantitative BLI research based on intravenous injection is limited, which greatly restricts the further application of BLI.

On the other hand, dynamic imaging followed by pharmacokinetic (PK) model analysis has more advantages than traditional static imaging [9, 10]. It can provide more information about the pharmacokinetic parameters of the probe, such as peak metabolic rates, clearance rates, binding potential and distribution volume [11]. In addition, when non-specific binding occurs, PK model can distinguish between specific and non-specific signals, which improve the accuracy of quantitative analysis [12-14]. Therefore, it is necessary to carry out quantitative research on dynamic BLI, especially on developing BLI for tumor growth prediction and drug efficacy evaluation.

In this study, a one-tissue (two-compartment) PK model suitable for BLI was designed under the precondition of intravenous low-dose injection. By using this model, we processed the dynamic BLI data and obtained two kinetic parameters associated with tumor uptake capacity. In addition,

Manuscript received April 29, 2018; revised June 14, 2018; accepted July 18, 2018. Date of publication XXXX, 2018; date of current version July 19, 2018. This work was partly supported by the National Natural Science Foundation of China (81627807, 81571725, 81530058, 11727813); Fok Ying-Tong Education Foundation of China (161104); Research Fund for Young Star of Science and Technology in Shaanxi Province (2018KJXX-018); Best Funded Projects for the Scientific and Technological Activities for Excellent Overseas Researchers in Shaanxi Province (2017017); Fundamental Research Funds for the Central Universities (JB171202, JB181203). *Asterisk indicates corresponding authors. Y. Dai and G. Wang contributed equally to this work.*

Y. Dai, D. Cheng, Y. Zhan, and J. Liang are with the Engineering Research Center of Molecular and Neuro Imaging of Ministry of Education & School of Life Science and Technology, Xidian University, Xi'an, Shaanxi 710071, China (e-mail: jimleung@mail.xidian.edu.cn).

G. Wang, J. Yin, Y. Nie, and K. Wu are with the State Key Laboratory of Cancer Biology and Xijing Hospital of Digestive Diseases, Xijing Hospital, Fourth Military Medical University, Xi'an 710032, China.

X. Chen is with the Engineering Research Center of Molecular and Neuro Imaging of Ministry of Education & School of Life Science and Technology, Xidian University, Xi'an, Shaanxi 710071, China. (e-mail: xlchen@xidian.edu.cn).

according to the relationship between the arterial input function (AIF) and the time activity curves of dynamic BLI derived from our PK model, we used a three exponential AIF to fit the time activity curves of dynamic BLI to obtain the time point of luminous intensity peak (TLP) [15]. Finally, the relationship between the obtained two kinetic parameters, the TLP values, and the tumor volume (TV) was compared and analyzed. The results imply that our PK model can predict tumor growth earlier and with higher sensitivity when compared to the conventional method, which may be significant for improving drug efficacy evaluation. In addition, our PK model may provide a valuable reference for noninvasive acquiring AIF, which may also provide a new application prospect for hybrid PET-optical imaging.

II. Materials and Methods

A. Experimental details

The care and treatment of animals in this study were performed in accordance with the Fourth Military Medical University (FMMU) animal protocol. Athymic male nude BALB/c mice (4 - 6 weeks, 18 - 22 g), were obtained from the Laboratory Animal Center, FMMU. Eight mice were randomly divided into two groups. The tumor was introduced by injecting $1*10^7$ MKN28M-luc gastric cancer cells insto the subcutaneous area of the shoulder in each mouse [16]. The tumor was allowed to grow for about three weeks before dynamic imaging. Data acquisition for dynamic BLI was performed by the IVIS Kinetic imaging system. On days 1, 3, 5, 7, and 9 of imaging, a 40-min dynamic BLI was carried out following intravenous injection of D-Luciferin at a dose of 2.5 mg/kg. The camera integration time was 1 s, and the frame rates were set to be 50 × 12 s and 60 × 30 s.

B. Pharmacokinetic model

When D-Luciferin is injected via the caudal vein, it is metabolized *in vivo* either by the kidney or other organs, or it is absorbed and decomposed by the tumor. If a larger dose of the substrate is maintained in the tumor region (that is, when the amount of the substrate metabolized at the early stage of the reaction is only a small fraction of the initial amount), its metabolic process in the tumor region satisfies the standard Michaelis–Menten (M-M) kinetics [17]. In this case, the two-tissue (three-compartment) PK model may be suitable to describe the metabolic process of the substrate *in vivo* according to the previous study [18]. The specific solving process can be found in Section *A* of Supplementary Materials. However, by intravenous injection, the metabolic rate of the substrate is very fast and it is difficult to maintain the dosage mentioned above throughout the collection process. In addition, it requires high amounts of substrate to be injected, which makes the process expensive.

Therefore, we injected a small dose of the substrate via the caudal vein, which led to rapid cycling and metabolism of the substrate. Further, we assumed that the amount of substrate in the tumor area quickly descends to relatively low levels, that is, the amount of substrate that enters the tumor area within the unit time is less and can be rapidly metabolized. At this point, the one-tissue (two-compartment) PK model is sufficient to describe the metabolic process of the substrate. As shown in Fig. 1, the model incorporates two parameters: (i) the non-metabolized D-Luciferin in the blood plasma (C_P), (ii) the metabolized D-Luciferin in the tumor region (C_S). K1 represents the substrate extravasation rate into the tumor region and k_{el} indicates the rate of substrate elimination in the plasma via other routes, such as through kidney filtration.

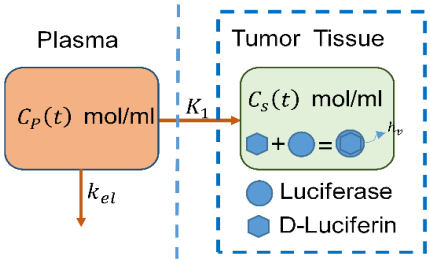

Fig. 1. Diagrammatic representation of the one-tissue (two-compartment) PK model.

The equations used to build the model depicted in Fig. 1 are as follows:

$$\frac{dC_P(t)}{dt} = -(K_1 + k_{el})C_P(t) \quad (1)$$

$$\frac{dC_S(t)}{dt} = K_1 C_P(t) \quad (2)$$

It should be noted that, according to the metabolic equation of D-luciferin, the time activity curve (TAC) of the BLI signal collected by the imaging instrument (set to $L(t)$) is proportional to the amount of the substrate in the tumor area that is metabolized within the unit time [8]. Therefore, we set the ratio to R, so that $C_S(t)$ should be equal to R multiplied by the time integral of $L(t)$. Then the relationship was expressed as:

$$C_S(t) = R\int L(t) \quad (3)$$

At the time of bolus injection, when the initial conditions of the above equation (Eq. (1) - Eq. (3)) are $C_P(0) \neq 0$ and $C_S(0) = 0$, and the results can be expressed as:

$$\int L(t) = A[1 - \exp(-K_B t)] \quad (4a)$$

where

$$A = \frac{K_1}{K_B R} C_P(0) \quad (4b)$$

$$K_B = K_1 + k_{el} \quad (4c)$$

The factor A and K_B are the parameters of interest, with A indicating the magnitude of the detected signal and K_B the sum of the kinetic rate constants (SKRC).

C. TLP Estimation

In addition, the relationship between the arterial input

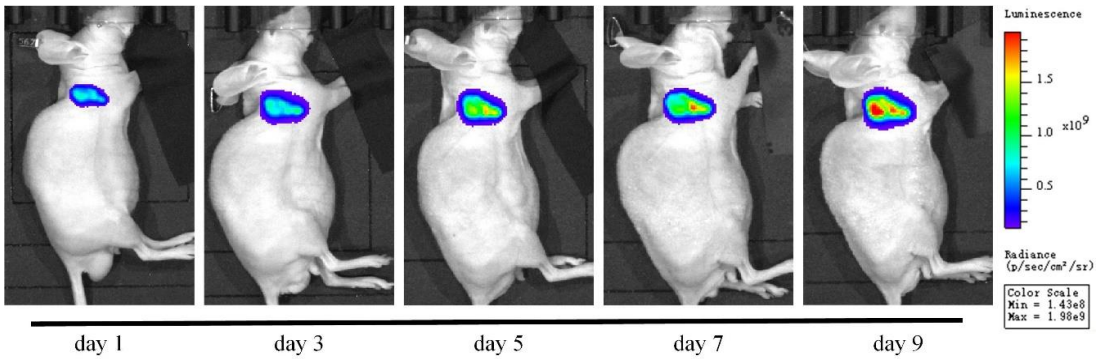

Fig. 2. Representative BLI results from days 1, 3, 5, 7 and 9 of imaging. The corresponding time points for each image were 2 min after the D-Luciferin injection, and all the images are displayed with the same color code.

function $C_P(t)$ and the TAC of the BLI signal $L(t)$ can be obtained by Eq. 2 and Eq. 3, which can be expressed as follows:

$$C_P(t) = \frac{R}{K_1} L(t) \tag{5}$$

It can be seen that the relationship between $C_P(t)$ and $L(t)$ is linear, thus the signal should be well fitted in the AIF model proposed by the Feng et al. [19]. At the same time, the TLP value of the TAC can also be estimated by this model.

D. Image and Data Analysis

Identification of the regions of interest (ROIs) in the tumor region and dynamic BLI data analysis were performed by the Living Image 4.5 software (PerkinElmer, USA) and MATLAB 2015b (The MathWorks, USA). For the quantitative analysis, ROIs of the tumors were determined in the white light images abided by a rule that the ROI should be entirely located within the circumference of the tumor. Although the placement and orientation of the mice may not be consistent in longitudinal observations, these will have no effects on the final quantitative results [8]. This is because the BLI signals would not be affected by the placement and orientation of the mice as long as the tumor can be seen completed by the detector. The mean values of the BLI signals (*10^6 photon/cm^2/s) in each ROI were calculated to determine the corresponding TACs in the tumor ROIs. In addition, data fitting was carried out using the Curve Fitting Toolbox in MATLAB and the goodness of fit was tested by the R-square value.

E. Statistic

Results were expressed as their mean values with standard deviations (means ± SD). Statistical significance was evaluated using one-way ANOVA; a least significant difference (LSD) test was used to control type II errors and carry out post-hoc testing to confirm pairwise significance. Differences with P values smaller than 0.05, were considered to be statistically significant.

III. Results

A. BLI results

Fig. 2 shows the representative longitudinal imaging results, all of which are displayed with the same color code at the corresponding dynamic BLI time points. It can be seen that the intensity and range of the BLI signals gradually increased over time, which suggests that the tumor is growing continuously.

B. PK results

The representative TACs of longitudinal imaging are shown in Fig. 3, which demonstrates that the corresponding area under the curve (AUC) and the peak of the TACs significantly increased over time, suggesting that the ability of tumor to absorb D-Luciferin is enhanced. The AIF model has an excellent fitting effect on the obtained TACs. In addition, there seemed to be no noticeable change in the corresponding time point of luminous intensity peak over time.

At the same time, the trend of TV values gradually increased with the passage of time. The corresponding statistical results are displayed in Fig. 4(a). The time point at which a significant statistical difference is observed is on day 7 compared to day 1 of imaging (LSD, $P < 0.05$). The statistical results of the TLP in longitudinal imaging are shown in Fig. 4(b). It can be seen that the TLP does not seem to have a distinct trend of change, and further statistical analysis shows that there is no significant

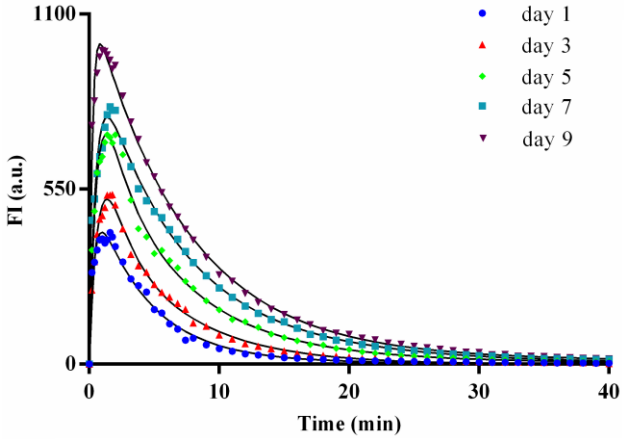

Fig. 3. Representative TACs of the BLI signal from days 1, 3, 5, 7 and 9 of imaging; the discrete points and solid lines respectively represent the raw BLI data obtained and the results of the fitting.

statistical difference between the groups (ANOVA, $P > 0.05$).

The representative integral TACs of longitudinal imaging are shown in Fig. 5. The corresponding asymptotic value of the

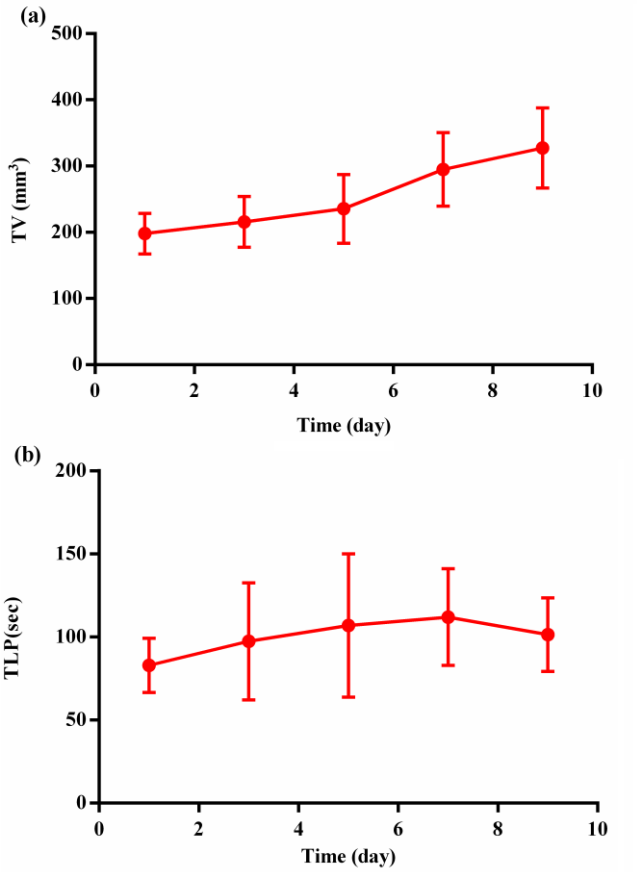

Fig. 4. Statistical results of the TV (a) and the TLP (b) trend in longitudinal imaging.

TACs significantly increased over time, which also implies an increase in tumor uptake. In addition, our model has a good fitting effect on the integral TACs of longitudinal imaging.

The corresponding statistical results of the A and K_B parameters in the model are shown in Fig. 6(a) and 6(b), respectively. As can be seen from Fig. 6(a), the A value increased over time, and on day 7 the difference became statistically significant when compared to day 1 of imaging (LSD, $P < 0.05$). However, the K_B value decreased over time, and there is statistically significant different between the groups

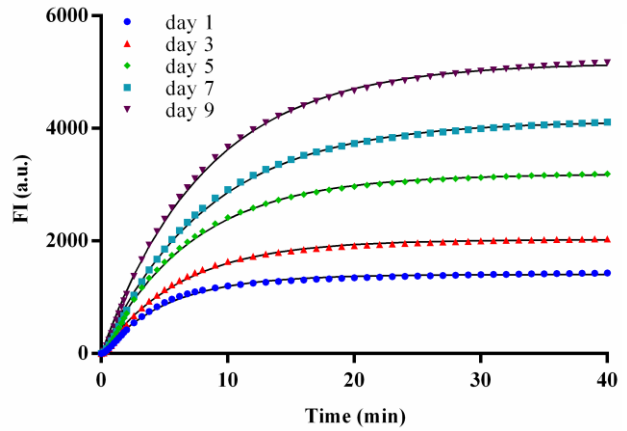

Fig. 5. Representative integral TACs of the BLI signal from days 1, 3, 5, 7 and 9 of imaging; the discrete points and solid lines respectively represent the raw BLI data obtained and the results of the fitting.

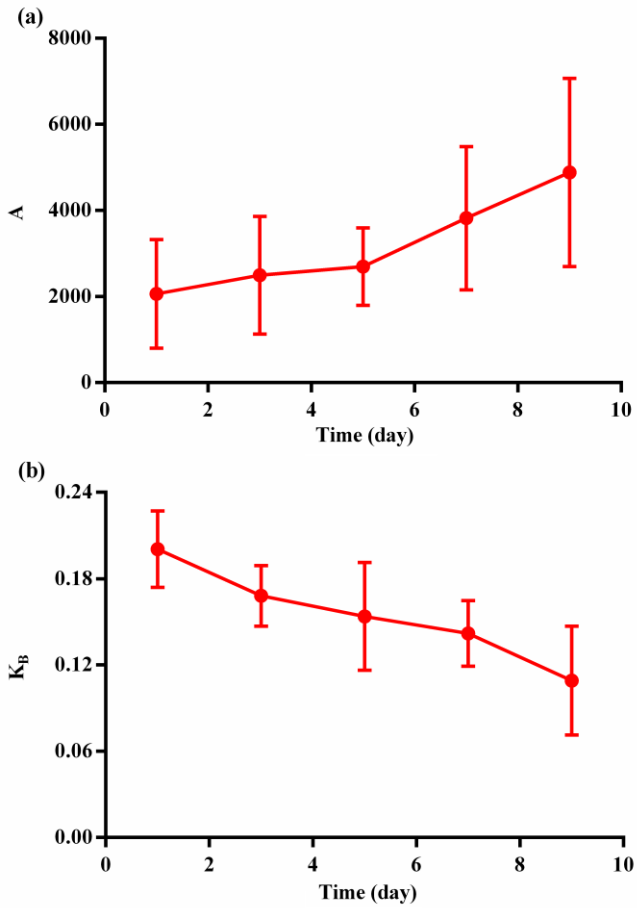

Fig. 6. Statistical results of the factor A (a) and the factor SKRC (b) trends in longitudinal imaging.

(LSD, $P < 0.05$).

IV. Discussion

Compared to the intraperitoneal or subcutaneous injection of the substrate, the metabolic process of the tail vein substrate injection has different hemodynamic characteristics [17, 20]. In this study, combined with the kinetic model constructed to apply on tail vein injection, the dynamic BLI was used to evaluate the tumor's growth. The results showed that the substrate injected via the tail vein had the characteristics of high luminous intensity and fast metabolism, so the dose needed for imaging was less and the process was more economical than the traditional static BLI. Dynamic BLI combined with the kinetic model presented in this study can provide more PK information, which can reflect the tumor's growth status earlier and with higher sensitivity, compared to the static method. In addition, unlike in intraperitoneal injection, it was found that TLP may not be an effective parameter to reflect the tumor's growth [8]. This may be due to the relatively short time it takes to reach the metabolic peak when the substrate is injected via the tail vein, which causes the TLP to be more sensitive to the error introduced by the operation or other factors.

The growth rate of different types of tumors may be varied, which may affect the injection dose of D-Luciferin. In previous studies, the typical injection dose for routine intraperitoneal injections is 150 mg/kg [21]; whereas the commonly used dose

for intravenous administration is 100 mg/kg [22]. In our study, in order to ensure the small dose injection of D-Luciferin, a dose of 2.5 mg/kg was used, which is much smaller than the commonly used values. Such small dose can enable the substrate to be metabolized faster in the tumor and then keep at a relatively low level that does not meet the M-M kinetics. This conforms to the hypothesis of the established model. Therefore, it can be seen from Fig. 5 that the kinetic model designed for this study can fit well the integral TACs. On the other hand, if the metabolic process of the substrate satisfies the M-M kinetics in the tumor region, the kinetic parameters obtained by using the constructed two-tissue (three-compartment) PK model to fit the integral TACs are not in a reasonable range. Even without considering the effective range of the kinetic parameters, the equation of the two-tissue (three-compartment) PK model can be simplified to that of the one-tissue (two-compartment) PK model according to the fitting parameters (see the Section A in Supplementary Materials).

In addition, it should be noted that the model used in this study ignores a PK parameter of k_2, which represents the substrate extravasation rate into the blood plasma from the tumor. This is because the amount of the substrate injection is small and the enzymatic reaction is very intense and fast. Therefore, the substrate that enters into tumor in unit time can be quickly consumed and would hardly return to the plasma. To confirm this statement, we also tested the fitting results of the model containing k_2, showing that the fitting results of two cases are almost identical. As a result, we can deduce that the k_2 is very small (see the Section *B* in Supplementary Materials). Although the PK model established in this study has a relatively small Akaike information criterion (AIC) value and provides less parameters, it is sufficient to effectively characterize the metabolic process of the substrate when a relatively low dose of substrate is injected by the caudal vein [23].

As can be seen from Fig. 6, the two PK parameters, A and K_B, can reflect the tumor's growth state effectively. In particular, K_B can predict tumor growth status earlier and with higher sensitivity, which is very important for drug development programs and monitoring the tumor's response to treatment. From Fig. 5, we can find that the ability of tumor to absorb the substrate gradually increases with its growth. This suggests that K_1 should increase as the tumor grows. From Eq. (4c), we can know that K_B equals K_1 plus k_{el}. Thus, only if k_{el} decreases with the growth of tumor, can K_B be reduced as the tumor grows. In other words, the ability of tumor to absorb substrate gradually increases as it grows, while the substrate metabolism of other organs decreases. Also, it is noteworthy that the value of A multiplied by K_B (equal to $C_p(0)K_1/R$) can be used as an effective PK parameter. The value of C_P *(0)* is related to the injection process, which can be regarded as constant relative to the value of R, therefore the value of $A*K_B$ may directly reflect the change of the PK parameter K_1. Because K_1 is directly related to the permeability and richness of tumor vessels, the value of $A*K_B$ may serve as an indicator of a tumor's angiogenesis state [24]. In addition, according to the kinetic model presented in this study, there is a linear relationship between the AIF and the TACs of the BLI signal. Furthermore, the three-exponential AIF model can be well fitted to the TACs of the BLI signal, which implies that dynamic BLI may provide useful reference information for obtaining AIF.

V. Conclusion

In this study we have demonstrated that dynamic BLI combined with the PK model established for tail vein injection, can be successfully used to quantitatively evaluate tumor growth. In addition, with our approach we can predict tumor growth earlier and with higher sensitivity than the conventional methods, which is crucial for drug development programs and monitoring the tumor's response to treatment. In addition, it may also provide a new application prospect for hybrid PET-optical imaging.

References

[1] D. Lambrechts et al, "Reporter cell activity within hydrogel constructs quantified from oxygen-independent bioluminescence," *Biomaterials*, vol. 35, no. 28, pp. 8065-77, 2014.

[2] T. Wurdinger et al, "A secreted luciferase for ex vivo monitoring of in vivo processes," *Nature Methods*, vol. 5, no. 2, pp. 171, 2008.

[3] A. Sato et al, "In vivo bioluminescence imaging," *Comparative Medicine*, vol. 54, no. 6, pp. 631-4, 2004.

[4] H. Tao et al , "In vivo NIR fluorescence imaging, biodistribution, and toxicology of photoluminescent carbon dots produced from carbon nanotubes and graphite," *Small*, vol. 8, no. 2, pp. 281-290, 2012.

[5] D. K. Welsh, and S. A. Kay, "Bioluminescence imaging in living organisms," *Current Opinion in Biotechnology*, vol. 16, no. 1, pp. 73-8, 2005.

[6] Y. D. R. D. L. Roy et al, "Kinetics of bactericidal activity of antibiotics measured by luciferin-luciferase assay," *Luminescence*, vol. 6, no. 3, pp. 193, 1991.

[7] W. X et al, " Dynamic tracking of human hematopoietic stem cell engraftment using in vivo bioluminescence imaging," *Blood*, vol. 102, no. 10, pp. 3478, 2003.

[8] H. Sim et al, "Pharmacokinetic modeling of tumor bioluminescence implicates efflux, and not influx, as the bigger hurdle in cancer drug therapy," *Cancer Research*, vol. 71, no. 3, pp. 686, 2011.

[9] Y. Dai et al, "Investigation of the influence of sampling schemes on quantitative dynamic fluorescence imaging," *Biomedical Optics Express*, vol. 9, no. 4, pp. 1859, 2018.

[10] N. Guo et al, "Quantitative analysis and parametric imaging of 18F-labeled monomeric and dimeric RGD peptides using compartment model," *Molecular Imaging & Biology*, vol. 14, no. 6, pp. 743-752, 2012.

[11] K. I. Shoghi, "Quantitative small animal PET," *The quarterly journal of nuclear medicine and molecular imaging*, vol. 53, no. 4, pp. 365, 2009.

[12] Y. Dai et al, "Investigation of injection dose and camera integration time on quantifying pharmacokinetics of a Cy5.5-GX1 probe with dynamic fluorescence imaging in vivo," *Journal of Biomedical Optics*, vol. 21, no. 8, pp. 86001, 2016.

[13] J. Guo et al, "(18)F-alfatide II and (18)F-FDG dual-tracer dynamic PET for parametric, early prediction of tumor response to therapy," *Journal of Nuclear Medicine Official Publication Society of Nuclear Medicine*, vol. 55, no. 1, pp. 154, 2014.

[14] Y. Dai et al, "In vivo quantifying molecular specificity of Cy5.5-labeled cyclic 9-mer peptide probe with dynamic fluorescence imaging," *Biomedical Optics Express*, vol. 7, no. 4, pp. 1149-1159, 2016.

[15] D. Vriens et al, "A curve-fitting approach to estimate the arterial plasma input function for the assessment of glucose metabolic rate and response to treatment," *Journal of Nuclear Medicine*, vol. 50, no. 12, pp. 1933-1939, 2009.

[16] R. Li et al, "Inhibition of CDH17 gene expression via RNA interference reduces proliferation and apoptosis of human MKN28 gastric cancer cells," *International Journal of Oncology*, vol. 50, no. 1, pp. 15, 2017.

[17] Y. Inoue et al, "Comparison of subcutaneous and intraperitoneal injection of D-luciferin for in vivo bioluminescence imaging," *European Journal of Nuclear Medicine & Molecular Imaging*, vol. 36, no. 5, pp. 771-779, 2009.

[18] M. Gurfinkel et al, "Quantifying molecular specificity of alphavbeta3 integrin-targeted optical contrast agents with dynamic optical imaging," *Journal of Biomedical Optics,* vol. 10, no. 3, pp. 034019, 2005.
[19] D. Feng et al, "Models for computer simulation studies of input functions for tracer kinetic modeling with positron emission tomography," *International Journal of Bio-Medical Computing,* vol. 32, no. 2, pp. 95-110, 1993.
[20] M. Keyaerts et al, "Dynamic bioluminescence imaging for quantitative tumour burden assessment using IV or IP administration of D-luciferin: effect on intensity, time kinetics and repeatability of photon emission," *European Journal of Nuclear Medicine & Molecular Imaging,* vol. 35, no. 5, pp. 999-1007, 2008.
[21] M. S. Evans et al, "A synthetic luciferin improves bioluminescence imaging in live mice," *Nature Methods,* vol. 11, no. 4, pp. 393-5, 2014.
[22] I. H. J. Ploemen et al, "Visualisation and quantitative analysis of the rodent malaria liver stage by real time imaging," *Plos One,* vol. 4, no. 11, pp. e7881, 2009.
[23] G. Z. Ferl et al, "Derivation of a Compartmental Model for Quantifying 64Cu-DOTA-RGD Kinetics in Tumor-Bearing Mice," *Journal of Nuclear Medicine Official Publication Society of Nuclear Medicine,* vol. 50, no. 2, pp. 250, 2009.
[24] R. E. Carson, "Tracer Kinetic Modeling in PET," vol. 2, no. 2, pp. 127-159, 2005.